

Research Article

An Algorithm of l_1 -Norm and l_0 -Norm Regularization Algorithm for CT Image Reconstruction from Limited Projection

Xiezhang Li,¹ Guocan Feng,² and Jiehua Zhu ¹

¹Department of Mathematical Sciences, Georgia Southern University, Statesboro 30460, USA

²School of Mathematics, Sun Yat-sen University, Guangzhou 510275, China

Correspondence should be addressed to Jiehua Zhu; jzhu@georgiasouthern.edu

Received 23 March 2020; Revised 1 June 2020; Accepted 6 July 2020; Published 28 August 2020

Academic Editor: Jyh-Cheng Chen

Copyright © 2020 Xiezhang Li et al. This is an open access article distributed under the Creative Commons Attribution License, which permits unrestricted use, distribution, and reproduction in any medium, provided the original work is properly cited.

The l_1 -norm regularization has attracted attention for image reconstruction in computed tomography. The l_0 -norm of the gradients of an image provides a measure of the sparsity of gradients of the image. In this paper, we present a new combined l_1 -norm and l_0 -norm regularization model for image reconstruction from limited projection data in computed tomography. We also propose an algorithm in the algebraic framework to solve the optimization effectively using the nonmonotone alternating direction algorithm with hard thresholding method. Numerical experiments indicate that this new algorithm makes much improvement by involving l_0 -norm regularization.

1. Introduction

Computed tomography (CT) has been widely applied in medical imaging and industry for over decades. In some applications, the reconstructions do not require a high-quality image, or complete projection data for exact reconstructions is not available because of the scanning conditions or radiation issue. CT reconstruction from limited projection data is of particular importance, and statistical and iterative reconstruction algorithms outperform the analytic approaches in these applications.

The theory of compressed sensing [1, 2] has provided a novel framework for CT image reconstruction from limited projection data with the prior knowledge of the sparse gradients for CT images. The total variation (TV) based regularization [3] for CT image reconstruction is connected to compressed sensing under the sparse transform of the gradient operator [4, 5]. The TV of an image is the l_1 -norm of the gradients of the image, so the TV minimization is also known as the l_1 -minimization.

The l_1 -norm-based regularization can greatly reduce the streak artifacts arising from few-view CT [6]. However, the results are over smoothing and lose some detailed features including contrast that causes edge blurred [7]. In addition,

the l_1 -norm regularization does not provide a representation sparse enough. To overcome the drawback, many improved TV-based reconstruction algorithms have been developed. One of them is the reweighted l_1 minimization [8]. Algorithms for regularization involving multiple norms are also developed. For example, the alternating direction method (ADM) [9, 10] and the nonmonotone alternating direction algorithm (NADA) [11, 12] are proposed for solving an l_1 -norm minimization with an l_2 -norm constraint.

The l_0 -norm of an image vector, defined as the number of its nonzero elements, measures the sparsity of a vector appropriately. So the l_0 -norm-based regularization for CT represents the sparsity of the gradient image better than the l_1 -norm-based regularization and preserves the edge while suppressing the streak artifacts [13]. However, the l_0 -norm is a nonconvex function and the l_0 -norm regularization problem is NP hard [14]. So many variants of the regularization algorithms are developed. An edge-preserving image reconstruction method for limited-angle CT is investigated based on l_0 -norm regularized gradient prior [15]. An imaging reconstruction model for few-view CT based on l_0 sparse regularization is proposed [16]. A new l_0 regularization with wavelet tight framelets is addressed to suppress the slope artifacts in the limited-

angle X-ray CT reconstruction [17]. Regularization involving multiple norms is also developed to address the individual drawbacks of the l_1 -norm and l_0 -norm. An image reconstruction model based on l_0 -norm and l_2 -norm regularization for the limited-angle CT is proposed [18]. Numerical experiments indicate that the algorithm has the advantage in suppressing slope artifacts. A combined smoothed l_0 -norm and l_1 -norm regularization algorithm using the NADA method for CT image reconstruction is proposed and demonstrated to have better performance than the l_1 -norm regularization [19].

In this paper, we will develop a new combined l_1 -norm and l_0 -norm regularization model for CT image reconstruction from limited projection data. The main contributions of this paper are as follows:

- (1) We generalize the l_1 -norm regularization to an l_1 -norm and l_0 -norm regularization for CT image reconstruction from limited projection data. The proposed model can achieve superior performance compared with the existing related methods for multiple reasons. Firstly, due to the l_1 -norm regularization term, the proposed model can reduce streak artifacts in limited-data CT. Secondly, due to the l_0 -norm regularization term, the oversmoothing from the l_1 -norm regularization term is improved. The proposed model is less smoothing, thus better edge-preserving, and provides a better sparsity representation. Thirdly, since the l_0 -norm is adopted without using the smoothed l_0 -norm approximation, the proposed model has the advantage in suppressing slope artifacts
- (2) We propose an algorithm in the algebraic framework to solve the optimization effectively using the non-monotone alternating direction algorithm with hard thresholding (NADA-HT) method

The rest of the paper is organized as follows. In Section 2, we present a combined l_1 -norm and l_0 -norm-based regularization model and propose an algorithm for CT image reconstruction from limited projection data. Numerical experiments for a comparison of regularization models with/without the l_0 -norm and the discussion are given in Section 3.

2. Materials and Methods

The projection data in CT can be modelled as a linear system,

$$\Phi f + e = u, \quad (1)$$

where Φ is an $m \times n^2$ projection matrix, $f \in R^{n^2}$ represents a 2D $n \times n$ image to be reconstructed, e an additive noise with $\|e\|_2 \leq \varepsilon$ for some known $\varepsilon > 0$, and $u \in R^m$ the noisy projection data. For limited data reconstruction, the underdetermined system ($m \ll n^2$) has infinitely many solutions. An optimal solution representing the original image as good as

possible can be sought by minimizing the energy function with a TV regularization term [8]:

$$\min_f \|f\|_{TV} \text{ subject to } \Phi f + e = u, \quad (2)$$

where the total variation $\|f\|_{TV}$ is the l_1 -norm of the magnitude of the discrete gradients,

$$\|f\|_{TV} = \|\nabla f\|_1 = \sum_{i,j} \sqrt{(f_{i+1,j} - f_{i,j})^2 + (f_{i,j+1} - f_{i,j})^2}. \quad (3)$$

Then, a 2D image f with sparse gradients and noisy measurements in CT can be reconstructed by solving the following l_1 -norm minimization with an l_2 -norm constraint,

$$\min_f \|\nabla f\|_1 \text{ subject to } \|\Phi f - u\|_2^2 \leq \varepsilon. \quad (4)$$

However, the image reconstructed by solving (4) has slope artifacts near the edge of the object for limited-angle projection data [20].

We consider the following minimization model

$$\min_f \left\{ \|\nabla f\|_1 + \alpha \|\nabla f\|_0 + \frac{\gamma}{2} \|f\|_2^2 \right\} \text{ subject to } \|\Phi f - u\|_2^2 \leq \varepsilon, \quad (5)$$

where $\|\nabla f\|_0$ stands for the number of nonzero gradients $(\nabla f)_p$, $1 \leq p \leq n^2$. The term $(\gamma/2)\|f\|_2^2$, $\gamma \rightarrow 0+$, makes the energy of reconstructed image to be minimized and reduces the ill-posedness of CT reconstruction [18].

For convenience, we denote $D_p f$ as the forward difference of f at a pixel p in both horizontal and vertical directions, i.e.,

$$D_p f = D_{i,j} f = [f_{i+1,j} - f_{i,j}, f_{i,j+1} - f_{i,j}]^T \in R^2, \text{ for } p = (i-1)n + j. \quad (6)$$

Then, $(\nabla f)_p = D_p f$ for $1 \leq p \leq n^2$ and $\|\nabla f\|_1 = \sum_{p=1}^{n^2} \|D_p f\|_2$.

Minimization (5) is equivalent to

$$\min_f \left\{ \frac{\beta}{2} \|\Phi f - u\|_2^2 + \sum_{p=1}^{n^2} (\|D_p f\|_2 + \alpha \|D_p f\|_0) + \frac{\gamma}{2} \|f\|_2^2 \right\}, \quad (7)$$

where the notation $\|D_p f\|_0$ is set to be 1 for nonzero $D_p f$, otherwise 0. The above minimization can be converted, with a parameter $\beta > 0$ and vectors v_p 's, to

$$\min_f \left\{ \frac{\beta}{2} \|\Phi f - u\|_2^2 + \sum_{p=1}^{n^2} \left(\|v_p\|_2 + \alpha \|v_p\|_0 \right) + \frac{\gamma}{2} \|f\|_2^2 \right\}$$

subject to $D_p f = v_p, 1 \leq p \leq n^2$.

(8)

Adapting Lagrangian vectors $\lambda_p \in \mathbb{R}^2, 1 \leq p \leq n^2$, we convert Minimization (8) into the following problem using the augmented Lagrangian method

$$\min_f \left\{ \frac{\beta}{2} \|\Phi f - u\|_2^2 + \sum_{p=1}^{n^2} \left(\|v_p\|_2 + \alpha \|v_p\|_0 \right) + \frac{\mu}{2} \|D_p f - v_p + \lambda_p\|_2^2 + \frac{\gamma}{2} \|f\|_2^2 \right\}.$$
(9)

For simplicity, we write Df , v , and λ as vectors whose p -th components are $D_p f$, v_p , and $\lambda_p, 1 \leq p \leq n^2$, respectively. Then, $\|Df - v + \lambda\|_2^2 = \sum_{p=1}^{n^2} \|D_p f - v_p + \lambda_p\|_2^2$. Thus, Minimization (9) becomes

$$\min_f \left\{ \frac{\beta}{2} \|\Phi f - u\|_2^2 + \sum_{p=1}^{n^2} \left(\|v_p\|_2 + \alpha \|v_p\|_0 \right) + \frac{\mu}{2} \|Df - v + \lambda\|_2^2 + \frac{\gamma}{2} \|f\|_2^2 \right\}.$$
(10)

Next, we will develop an algorithm for solving Minimization (10). By convention, Minimization (10) can be solved by ADM iteratively. The k -th step of the ADM involves three procedures,

$$f^{k+1} \in \arg \min_f \left\{ \frac{\beta}{2} \|\Phi f - u\|_2^2 + \frac{\mu}{2} \|Df - v^k + \lambda^k\|_2^2 + \frac{\gamma}{2} \|f\|_2^2 \right\},$$
(11)

$$v^{k+1} \in \arg \min_v \left\{ \sum_{p=1}^{n^2} \left(\|v_p\|_2 + \alpha \|v_p\|_0 \right) + \frac{\mu}{2} \|Df^{k+1} - v + \lambda^k\|_2^2 \right\},$$
(12)

$$\lambda^{k+1} = \lambda^k - \left(v^{k+1} - Df^{k+1} \right).$$
(13)

First, Minimization (11) can be solved by ADM with the gradient decent method involving nonmonotone line search, for example, the NADA.

Next, we seek for a solution of (12). Minimization (12) is equivalent to finding

$$v_p^{k+1} \in \arg \min_{v_p} \left\{ \|v_p\|_2 + \alpha \|v_p\|_0 + \frac{\mu}{2} \|D_p f^{k+1} - v_p + \lambda_p^k\|_2^2 \right\}, \text{ for } 1 \leq p \leq n^2.$$
(14)

We introduce a hard thresholds (HT) operator $H_\kappa(w)$ on \mathbb{R}^2 with the threshold κ defined as

$$H_\kappa(w) = \begin{cases} 0 & \text{if } \|w\|_2 \leq \kappa \\ w & \text{otherwise.} \end{cases}$$
(15)

A solution v_p^{k+1} is provided in the following theorem.

Theorem 1. Let $w = D_p f^{k+1} + \lambda_p^k$ and $\kappa = (1/\mu)(1 + \sqrt{2\mu\alpha})$. If $2\mu\alpha > 1$, then a minimizer v_p^{k+1} for Minimization (14) is given by

$$v_p^{k+1} = \max \left\{ 1 - \frac{1}{\mu\|w\|_2}, 0 \right\} H_\kappa(w).$$
(16)

Proof. For simplicity, denote $z = v_p$. The objective function in Minimization (14) is rewritten as

$$g(z) = \|z\|_2 + \alpha \|z\|_0 + \frac{\mu}{2} \|z - w\|_2^2.$$
(17)

Without loss of generality, we assume that $w \neq 0$ since $z_{opt} = 0$ in the case of $w = 0$.

For $z = 0$, $g(z) = (\mu/2)\|w\|_2^2$.

For $z \neq 0$, $g(z) = \|z\|_2 + \alpha + (\mu/2)\|z - w\|_2^2$. The minimizer is derived in the following two cases.

(i) Case 1. $\mu\|w\|_2 > 1$

We claim that $g_{\min} = \|w\|_2 + \alpha - 1/(2\mu)$ at $z = (1 - 1/(\mu\|w\|_2))w$. In fact, it follows from

$$\frac{dg}{dz} = \frac{1}{\|z\|_2} z + \mu(z - w) = 0$$
(18)

that a minimizer z is a scalar multiple of w . Let $z = tw$ where $t > 0$ due to the minimization problem. Then, the function

$$\begin{aligned} h(t) &:= g(z) = \frac{\mu}{2} \|tw - w\|_2^2 + \|tw\|_2 + \alpha \\ &= \frac{\mu}{2} \|w\|_2^2 t^2 - (\mu\|w\|_2^2 - \|w\|_2)t + \frac{\mu}{2} \|w\|_2^2 + \alpha \end{aligned}$$
(19)

reaches its minimum value

$$h_{\min} = \alpha + \frac{\mu}{2} \|w\|_2^2 - \frac{(\mu\|w\|_2^2 - \|w\|_2)^2}{2\mu\|w\|_2^2} = \alpha + \|w\|_2 - \frac{1}{2\mu}$$
(20)

at $t = 1 - 1/(\mu\|w\|_2)$. The claim is proved.

(ii) Case 2. $\mu\|w\|_2 \leq 1$

```

( $l_1$ -norm and  $l_0$ -norm regularization algorithm using NADA-HT method).
1. input  $\Phi, u, \alpha, \varepsilon$ 
2. initialize  $n, \beta, \gamma, \mu, k, f^0, v^0, \lambda^0, maxit, ratio, tol$ 
3. while  $k < maxit$ 
3.1 update  $f^{k+1}$  by NADA
3.2 for each integer  $p, 1 \leq p \leq n^2$ , update  $v_p^{k+1}$  by HT method
      set  $w = D_p f^{k+1} + \lambda_p^k, \kappa = (1/\mu)(1 + \sqrt{2\mu\alpha})$ 
      update  $v_p^{k+1} = \max \{1 - 1/(\mu\|w\|_2), 0\} H_\kappa(w)$ 
3.3 update  $\lambda^{k+1} = \lambda^k + (Df^{k+1} - v^{k+1})$ 
3.4 if error  $< tol$  then output  $f^{k+1}$ ; stop
3.5  $\gamma = \gamma \times ratio$ 
3.6  $k = k + 1$ 
end.

```

ALGORITHM 1.

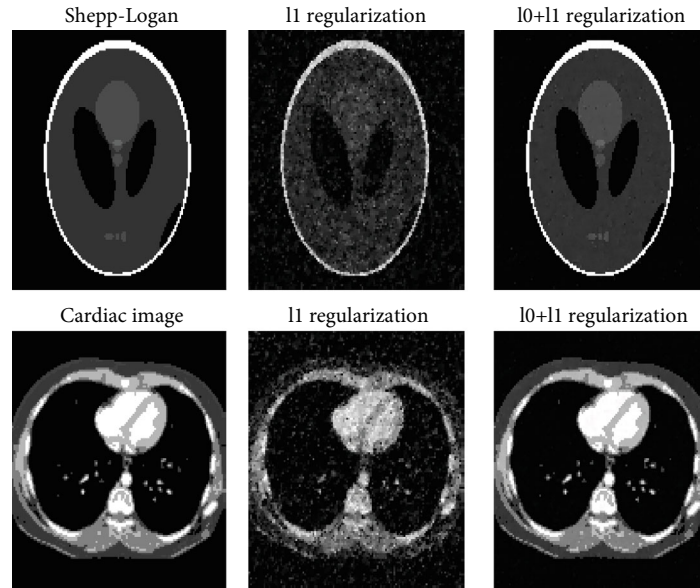


FIGURE 1: Original and reconstructed images. First row: Shepp-Logan phantom after 200 iterations. Second row: cardiac image after 500 iterations.

In this case, $h'(t) = \mu\|w\|_2^2(t - 1/(\mu\|w\|_2)) > 0$ for all $t > 0$ and $\lim_{t \rightarrow 0^+} h(t) = (\mu/2)\|w\|_2^2 + \alpha > (\mu/2)\|w\|_2^2$. Thus, the minimizer is $z_{opt} = 0$.

Combining the results for $z = 0$ and $z \neq 0$, we conclude that if $(\mu/2)\|w\|_2^2 \leq \alpha + \|w\|_2 - 1/(2\mu)$ then, $z_{opt} = 0$; otherwise, $z_{opt} = \max \{1 - 1/(\mu\|w\|_2), 0\}w$.

Next, we look for conditions under which the inequality $(\mu/2)\|w\|_2^2 \leq \alpha + \|w\|_2 - 1/(2\mu)$ holds. Substituting $r = \|w\|_2$ into the inequality, we consider the equation

$$q(r) := \frac{\mu}{2}r^2 - r - \left(\alpha - \frac{1}{2\mu}\right) = 0 \quad (21)$$

in an unknown r . The zeros of the equation are given by $r_{1,2} = (1/\mu)(1 \mp \sqrt{2\mu\alpha})$. So $q(r) \leq 0$ for $r \in [r_1, r_2]$, where

$r_1 \leq 0$ for $2\mu\alpha > 1$, and $q(r) > 0$ for $r > r_2$. Therefore, for $2\mu\alpha > 1$, if $\|w\|_2 \leq (1/\mu)(1 + \sqrt{2\mu\alpha})$, we have $(\mu/2)\|w\|_2^2 \leq \alpha + \|w\|_2 - 1/(2\mu)$, and consequently, $z_{opt} = 0$; otherwise, $(\mu/2)\|w\|_2^2 > \alpha + \|w\|_2 - 1/(2\mu)$, and consequently, $z_{opt} = \max \{1 - 1/(\mu\|w\|_2), 0\}w$.

With a threshold $\kappa = (1/\mu)(1 + \sqrt{2\mu\alpha})$, if $\|w\|_2 \leq \kappa$, then $z_{opt} = 0$; otherwise, $z_{opt} = \max \{1 - 1/(\mu\|w\|_2), 0\}w$. Using the HT operator in (14), we have $z_{opt} = \max \{1 - 1/(\mu\|w\|_2), 0\}H_\kappa(w)$. We complete the proof of the theorem.

Remark. In practice, the condition $2\mu\alpha > 1$ for nonzero α in Theorem 1 is fulfilled. Now we summarize our algorithm as follows.

3. Results and Discussion

In this section, the performance of the proposed algorithm is compared with that of the l_1 -norm regularization algorithm.

TABLE 1: Comparison of two algorithms after same number of iterations.

(a)

Shepp-Logan phantom, after 200 iterations						
	Time(s)	Error	RMSE	NRMSD	NMAD	SSIM
l_1 regularization	53	0.341	0.083	0.086	0.422	0.356
$l_0 + l_1$ regularization	52	0.035	0.009	0.009	0.033	0.949

(b)

Cardiac image, after 500 iterations						
	Time(s)	Error	RMSE	NRMSD	NMAD	SSIM
l_1 regularization	88	0.362	0.111	0.076	0.352	0.442
$l_0 + l_1$ regularization	83	0.119	0.014	0.010	0.041	0.936

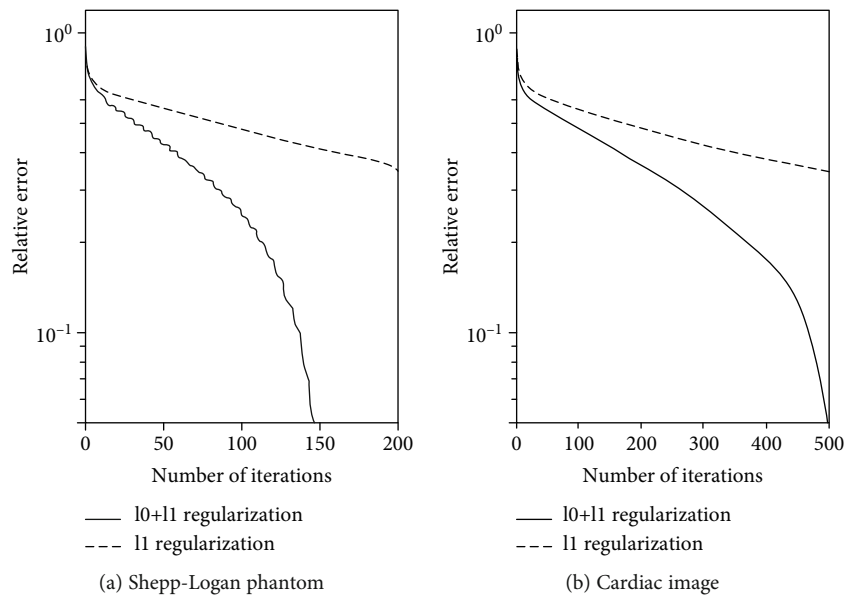


FIGURE 2: Relative error v.s. iteration number in reconstruction by two algorithms. (a) Shepp-Logan phantom. (b) Cardiac image.

Both algorithms are implemented in MATLAB using the NADA and tested with the 2D Shepp-Logan phantom and a cardiac image [21] of size 128×128 on an Intel Core i7 3.40 GHz PC. In each test, the same system $u = \Phi f + e$ is created, where $\Phi \in R^{m \times n^2}$ ($m \approx 0.3n^2$) is a random matrix and the noise $e = 0.02 * \text{mean}(\Phi f) * \text{randn}(m)$. The weight parameter α is chosen as 0 and 1 for the l_0 -norm regularization and the proposed algorithm, respectively. Other two important parameters in the objective function are taken as $\beta = 2^8$, $\mu = 2^4$ for the Shepp-Logan phantom and $\beta = 2^7$, $\mu = 2^2$ for the cardiac image, respectively.

Experiments are conducted to compare the reconstruction by the two algorithms after the same number of iterations. The original and reconstructed images for two images after the same numbers of iterations are shown in Figure 1. The images demonstrate that the proposed algorithm yields much better reconstruction. The quality of reconstructed images is compared using several commonly used criteria: the relative error, the root-mean-square error (RMSE), the normalized root mean square deviation (NRMSD), the nor-

malized mean absolute deviation (NMAD), and the structural similarity index (SSIM). The experimental results from 100 tests are summarized in Table 1. It shows that the proposed algorithm produces significantly improved evaluation measurement: 88%–167% for the Shepp-Logan phantom and 67%–114% for the cardiac image, respectively, while taking less CPU time. Overall, the new algorithm provides better accuracy after the same iteration number.

Figure 2 shows the graph of relative error v.s. the number of iterations for the two algorithms. The curves indicate that the proposed algorithm requires much less iterations and time to achieve the same accuracy and yields much faster convergence. After a certain number of iteration numbers, the relative error of the proposed algorithm drops sharply, while the relative error of the l_1 -norm regularization is slowly decreasing and does not improve much over the iterations.

The proposed regularization model introduces an l_0 -norm term in addition to an l_1 -norm term. The l_0 -norm of a vector is the number of nonzero elements in the vector; thus, the l_0 -norm is appropriate for representing sparsity.

Meanwhile, the l_0 -norm term makes the model less smoothing. Numerical experiments demonstrate that, in the proposed model, the edge is better preserved, and a better sparsity representation is provided. So, the proposed algorithm improves the quality and the efficiency of the reconstruction even with the extra computation from the added l_0 -norm term.

The effect of the weight parameter α of the l_0 -norm is tested. From our experiments, the parameter α from 0.5 to 1 almost does not affect the efficiency of the algorithm. Selecting good values of other parameters β , μ , and γ in Minimization (10) is a challenging problem and will be further investigated in the future.

High-quality CT image reconstruction from limited projection data is challenging. Learning based algorithms such as structure-aware sparse Bayesian learning [22] could yield improved performance in reconstructing tomographic images from limited data, since structural prior knowledge is exploited. Enhancing the proposed algorithm in a learning-based framework using prior knowledge will be the topic of future research.

Data Availability

The data used to support the findings of the study included within the article.

Conflicts of Interest

The authors declare that there is no conflict of interest regarding the publication of this paper.

Acknowledgments

The authors would like to thank the reviewers and editors for their valuable comments and suggestions. It is acknowledged that G. Feng was partially supported by the National Natural Science Foundation of China (NSFC) under grant No. 61673018.

References

- [1] E. Candes and W. Wakin, "An introduction to Compressive sampling," *IEEE Signal Processing Magazine*, vol. 25, no. 2, pp. 21–30, 2008.
- [2] C. E. Shannon, "Communication in the presence of noise," *Proceedings of the IEEE*, vol. 86, no. 2, pp. 447–457, 1998.
- [3] L. I. Rudin, S. Osher, and E. Fatemi, "Nonlinear total variation based noise removal algorithms," *Physica D*, vol. 60, no. 1–4, pp. 259–268, 1992.
- [4] E. J. Candes, J. Romberg, and T. Tao, "Robust uncertainty principles: exact signal reconstruction from highly incomplete frequency information," *IEEE Transactions on Information Theory*, vol. 52, no. 2, pp. 489–509, 2006.
- [5] D. Donoho, "Compressed sensing," *IEEE Transactions on Information Theory*, vol. 52, no. 4, pp. 1289–1306, 2006.
- [6] H. Yu and G. Wang, "Compressed sensing based interior tomography," *Physics in Medicine and Biology*, vol. 54, no. 9, pp. 2791–2805, 2009.
- [7] Z. Tian, X. Jia, K. Yuan, T. Pan, and S. B. Jiang, "Low-dose CT reconstruction via edge-preserving total variation regularization," *Physics in Medicine and Biology*, vol. 56, no. 18, pp. 5949–5967, 2011.
- [8] E. Candes, W. Wakin, and S. Boyd, "Enhancing Sparsity by Reweighted l_1 Minimization," *Journal of Fourier Analysis Application*, vol. 14, no. 5–6, pp. 877–905, 2008.
- [9] M. Tao and J. Yang, *Alternating direction algorithms for total variation deconvolution in image reconstruction*, Optimization Online, 2009.
- [10] J. Yang and Y. Zhang, "Alternating direction algorithms for l_1 -problems in compressive sensing," *SIAM Journal on Scientific Computing*, vol. 33, no. 1, pp. 250–278, 2011.
- [11] C. Li, W. Yin, H. Jiang, and Y. Zhang, "An efficient augmented Lagrangian method with applications to total variation minimization," *Computational Optimization and Applications*, vol. 56, no. 3, pp. 507–530, 2013.
- [12] C. Li, W. Yin, and Y. Zhang, *User's Guide for TVAL3: TV Minimization by Augmented Lagrangian and Alternating Direction Algorithms*, CAAM Report, 2010.
- [13] W. Yu and L. Zeng, " l_0 gradient minimization based image reconstruction of limited angle computed tomography," *PLOS ONE*, vol. 10, no. 7, 2015.
- [14] B. Natarajan, "Sparse approximate solutions to linear systems," *SIAM Journal on Computing*, vol. 24, no. 2, pp. 227–234, 1995.
- [15] W. Yu, C. Wang, and M. Huang, "Edge-preserving reconstruction from sparse projections of limited-angle computed tomography using l_0 -regularized gradient prior," *Review of Scientific Instruments*, vol. 88, no. 4, p. 043703, 2017.
- [16] W. Yu, C. Wang, X. Nie, M. Huang, and L. Wu, "Image reconstruction for few-view computed tomography based on l_0 sparse regularization," *Procedia Computer Science*, vol. 107, pp. 808–813, 2017.
- [17] L. Zhang, L. Zeng, and Y. Guo, " l_0 regularization based on a prior image incorporated non-local means for limited-angle X-ray CT reconstruction," *Journal of X-Ray Science and Technology*, vol. 26, no. 3, pp. 481–498, 2018.
- [18] C. Wang, L. Zeng, W. Yu, and L. Xu, "Existence and convergence analysis of l_0 and l_2 regularizations for limited-angle CT reconstruction," *Inverse Problems and Imaging*, vol. 12, no. 3, pp. 545–572, 2018.
- [19] J. Zhu and X. Li, "A Smoothed l_0 -norm and l_1 -norm Regularization Algorithm for Computed Tomography," *Journal of Applied Mathematics*, vol. 2019, Article ID 8398035, 8 pages, 2019.
- [20] L. Zeng, J. Guo, and B. Liu, "Limited-angle cone-beam computed tomography image reconstruction by total variation minimization," *Journal of Inverse and Ill-Posed Problems*, vol. 21, no. 6, pp. 735–754, 2013.
- [21] TEAM RADS <http://teamrads.com/>.
- [22] S. Liu, Y. Huang, H. Wu, C. Tan, and J. Jia, "Efficient multi-task structure-aware sparse Bayesian learning for frequency-difference electrical impedance tomography," *IEEE Transactions on Industrial Informatics*, vol. 16, p. 1, 2020.